

Supporting Information

"Old dog, new tricks": the lone pair effect inducing divergent optical responses in lead cyanurates containing π -bonds

Xianghe Meng,^{a,d,#} Kaijin Kang,^{b,c,#} Fei Liang,^{a,#} Jian Tang,^{b,c} Zheshuai Lin,^a Wenlong Yin,^{*b} and Mingjun Xia^{*a,d}

^a Beijing Center for Crystal Research and Development, Key Laboratory of Functional Crystals and Laser Technology, Technical Institute of Physics and Chemistry, Chinese Academy of Sciences, Beijing 100190, China.

Email: xiamingjun@mail.ipc.ac.cn.

^b Institute of Chemical Materials, China Academy of Engineering Physics, Mianyang 621900, China. E-mail: wlyin@caep.cn

^c Physics and Space Science College, China West Normal University, Nanchong 637002, China

^d Center of Materials Science and Optoelectronics Engineering, University of Chinese Academy of Sciences, Beijing 100049, China

Table of Contents

Experimental Procedures

1. Synthesis
2. Powder X-ray diffraction
3. UV–vis–NIR diffuse reflectance spectrum
4. Infrared spectrum
5. Thermal analysis
6. Single crystal structure determination
7. Computational methods

Result and discussion

Figure S1. Experimental powder XRD spectra of (a) I and (b) II

Figure S2. TG curves for I and II

Figure S3. Experimental infrared spectrum of I

Figure S4. Band structures of I and II

Figure S5. Density of states of I and II

Table S1. Crystal data and structure refinements for I and II

Table S2. Fractional atomic coordinates, equivalent isotropic displacement parameters (\AA^2) for I and II

Table S3. Selected bond lengths (\AA) and angles (degree) for I and II

References

Experimental procedures

Synthesis. All chemicals containing Pb(OH)_2 (Macklin, $\geq 98\%$), Cd(OH)_2 (Macklin, 98.5%) and $\text{H}_3\text{C}_3\text{N}_3\text{O}_3$ (Aladdin, 98%) were used without further purification and their dissolution in deionized water took place in air.

Single crystals of I and II were synthesized by hydrothermal methods. The mixture of Pb(OH)_2 , $\text{H}_3\text{C}_3\text{N}_3\text{O}_3$ with a molar ratio of 3:2 in H_2O (8.0 mL) was sealed in an autoclave with a Teflon liner (23 mL) and heated at 130 °C for 12 hours, which was slowly cooled to room temperature at a rate of 2°C/h. Under the same conditions, II was synthesized from Pb(OH)_2 , Cd(OH)_2 , $\text{H}_3\text{C}_3\text{N}_3\text{O}_3$ with a molar ratio of 2:1:2 in H_2O (8.0 mL). Colorless and transparent crystals with regular shapes were obtained after washing with deionized water and ethanol.

Powder X-ray diffraction. The powder X-ray diffraction (PXRD) data of the target samples were successfully collected on Bruker D8 Focus diffractometer equipped with Cu K α radiation ($\lambda=1.5418 \text{ \AA}$) in the 2θ range of 5-70° at room temperature.

UV-vis-NIR diffuse reflectance spectrum. The UV-vis-NIR diffuse reflectance spectra were measured in the wavelength range from 200 nm to 2000 nm with BaSO_4 as a reference material by Cary 7000 UV-vis-NIR universal measurement spectrophotometer under an integrating sphere.

IR spectrum. FTIR spectrum of I was collected on a Varian Excalibur 3100 spectrometer in the 400 - 4000 cm^{-1} range. I and KBr samples were mixed thoroughly with mass ratio about 1:100, respectively.

Thermal analysis. Thermal gravimetric analysis (TGA) were carried out on NETZSCH STA 409 CD thermal analyzer at a temperature range of 100-550 °C and 100-600 °C for I and II respectively with a heating rate of 10 K/min in nitrogen atmosphere.

Single crystal structure determination. The single-crystal X-ray diffraction data was gathered on a Rigaku AFC10 single-crystal diffractometer equipped with graphite-monochromatic Mo K α radiation ($\lambda= 0.71073 \text{ \AA}$) and Saturn CCD detector at 293 K.

The intensity data, data reduction and cell refinement were captured by the CrystalClear program. The crystal structures were settled by the direct method with program SHELXS-97 and further refined by full matrix least squares on F^2 by SHELXL-97 programs. The structure was confirmed by using the ADDSYM algorithm from the program PLATON with no higher symmetry discovered. The crystallographic data are given in Table S1 - 3.

Computational methods.

Notably, a similar chemical formula $\text{Pb}_3\text{O}_2(\text{O}_3\text{C}_3\text{N}_3\text{H}_2)_2$ with non-centrosymmetric Cc space group has been reported by Meyer's group in 2015.¹ We checked these two structures carefully and identity the refined structure in this work is indeed accurate. So, all following calculations are based on this experimental structure without any optimizations. The theoretical calculations for isostructural $\text{Pb}_3(\text{HC}_3\text{N}_3\text{O}_3)_2(\text{OH})_2$ and $\text{Pb}_2\text{Cd}(\text{HC}_3\text{N}_3\text{O}_3)_2(\text{OH})_2$ were performed by *ab initio* density functional theory² on basis of CASTEP module.³ In early reports, this method has been applied on H-free metal cyanurates as well as hydro-cyanurates successfully.⁴⁻¹² The exchange–correlation (XC) functional was modeled by the generalized gradient density approximation (GGA)¹³ and the norm-conserving pseudopotentials¹⁴ were applied for all elements. In this model, Pb $6s^26p^2$, Cd $5s^24p^64d^{10}$, C $2s^22p^2$, N $2s^22p^3$, O $2s^22p^4$ and H $1s$ electrons were modeled as the outer valence electrons, respectively. The kinetic energy cutoff of 900 eV and dense k -point meshes¹⁵ ($2 \times 4 \times 2$) in the first Brillouin zone were chosen to guarantee the sufficient calculation accuracy.

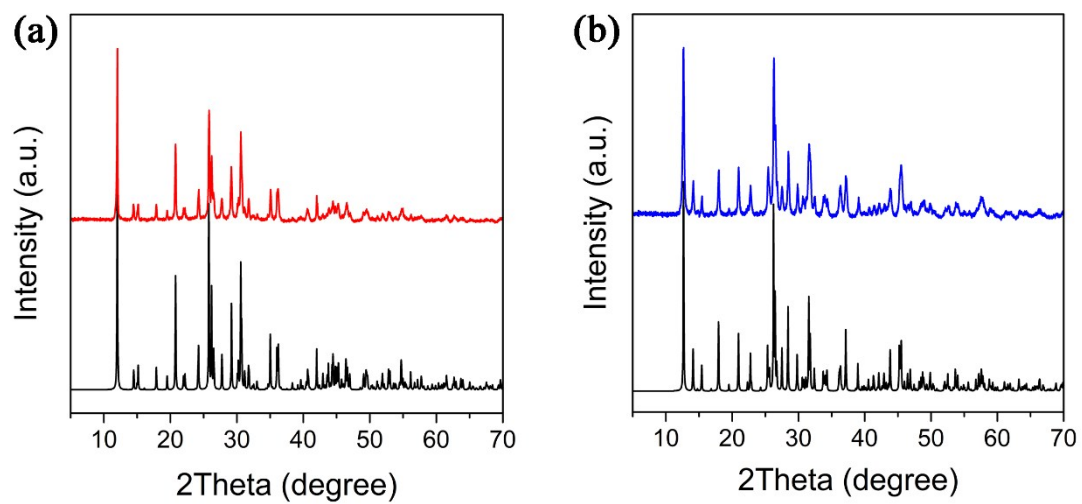


Figure S1. Experimental powder XRD spectra of (a) I and (b) II

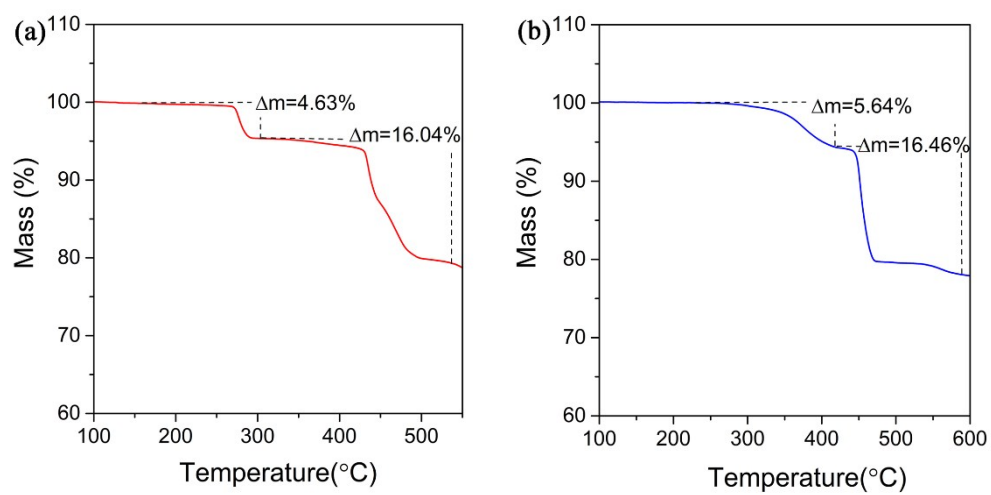


Figure S2. The TG curves for (a) I and (b) II

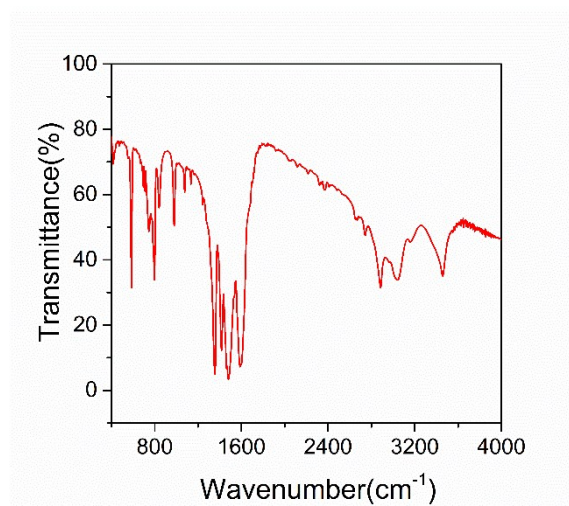


Figure S3. The IR spectrum of I

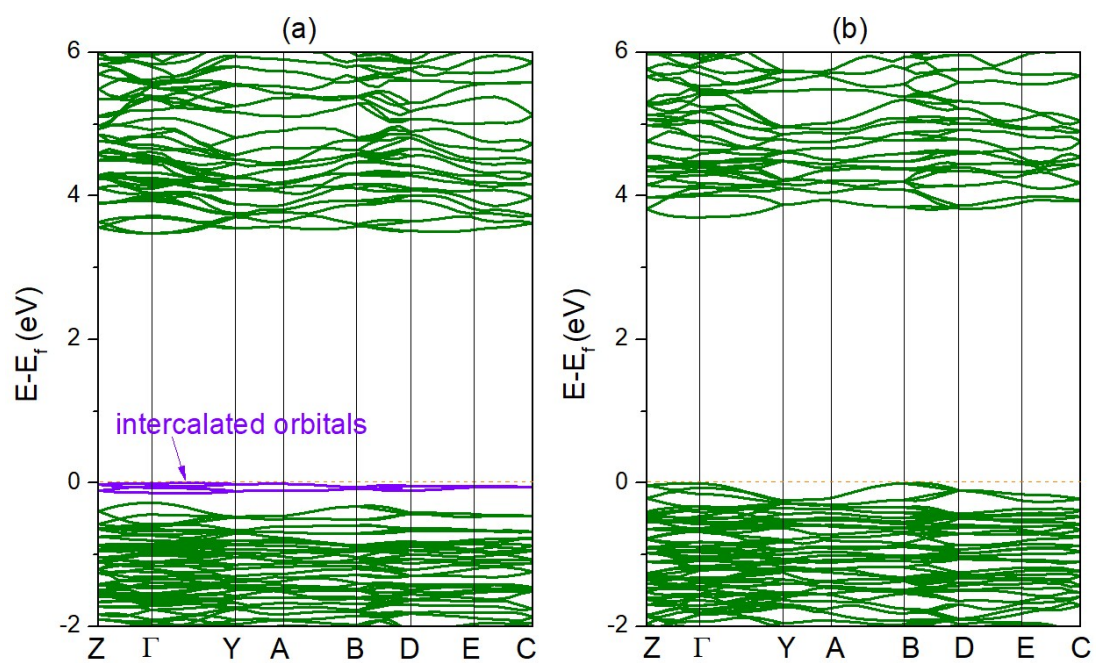


Figure S4. Calculated band structure calculated by PBE functional, (a) I and (b) II

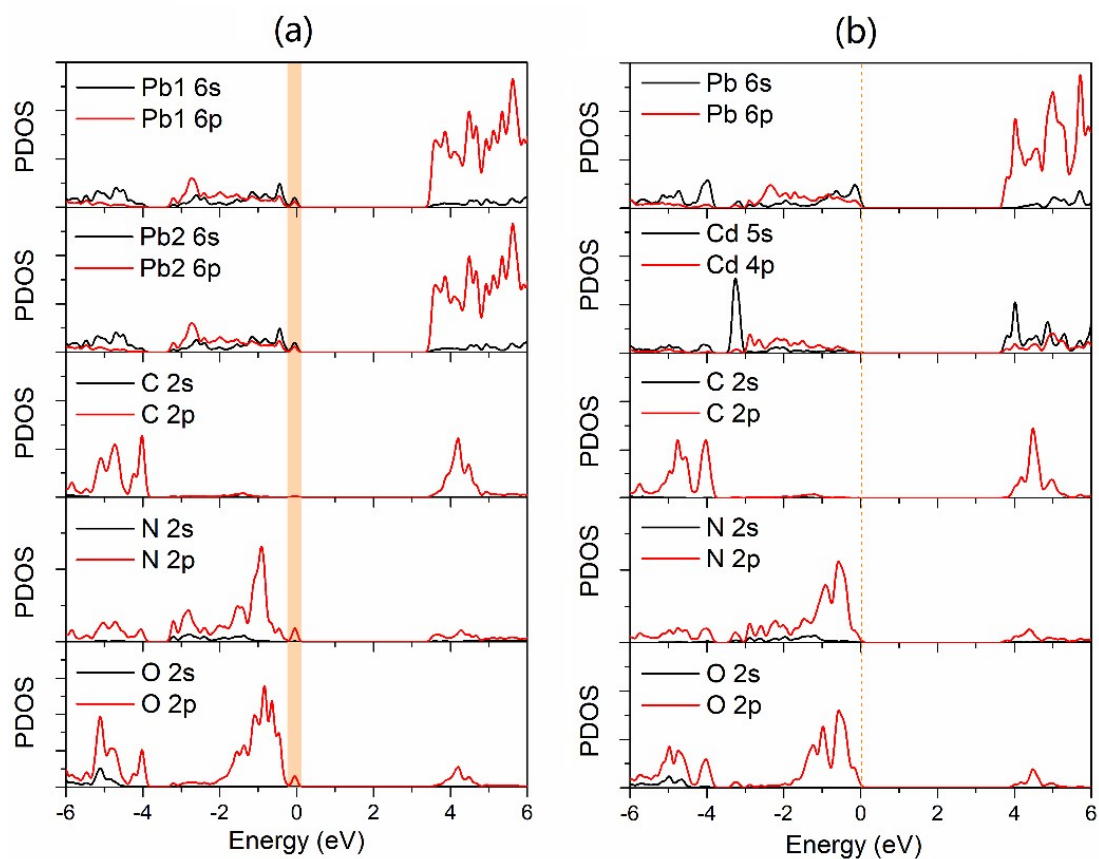


Figure S5. The partial density of states projected constituent atoms of (a) I and (b) II. The contribution from hydroxyl molecule was omitted for simplification.

Table S1. Crystal data and structure refinements for I and II

Chemical formula	I	II
Formula weight	909.72	814.93
Temperature/K	293	293
Crystal system	monoclinic	monoclinic
Space group	<i>C2/c</i>	<i>C2/c</i>
<i>a</i> /Å	16.6034 (11)	15.9504 (12)
<i>b</i> /Å	6.7166 (3)	7.0252 (4)
<i>c</i> /Å	12.4132 (6)	12.0267 (8)
α /°	90	90
β /°	117.563 (6)	118.914 (7)
γ /°	90	90
Volume/Å ³	1227.19 (11)	1179.66 (14)
<i>Z</i>	4	4
<i>R</i> _{int}	0.035	0.035
ρ_{calc} g/cm ³	4.924	4.589
μ /mm ⁻¹	41.12	30.32
<i>F</i> (000)	1568	1432
Goof on <i>F</i> ²	1.111	1.062
Final <i>R</i> indexes [<i>I</i> ≥2σ (<i>I</i>)]	<i>R</i> ₁ = 0.0194, <i>wR</i> ₂ = 0.0448	<i>R</i> ₁ = 0.0181, <i>wR</i> ₂ = 0.0448
Final <i>R</i> indexes [all data]	<i>R</i> ₁ = 0.0203, <i>wR</i> ₂ = 0.0451	<i>R</i> ₁ = 0.0197, <i>wR</i> ₂ = 0.0455

$$^a R_1 = \frac{\sum ||F_o| - |F_c||}{\sum |F_o|} \text{ and } wR_2 = \frac{\left[\sum [w(F_o^2 - F_c^2)^2] \right]^{1/2}}{\left[\sum [w(F_o^2)^2] \right]^{1/2}} \text{ for } F_o^2 > 2\sigma(F_c^2)$$

Table S2. Fractional atomic coordinates, equivalent isotropic displacement parameters (\AA^2) for I and II

I				
	<i>x</i>	<i>y</i>	<i>z</i>	$U_{\text{iso}}^*/U_{\text{eq}}$
Pb1	1.062308 (12)	1.20157 (3)	0.609544 (16)	0.01761 (9)
Pb2	1.0000	0.72291 (4)	0.7500	0.01499 (9)
C1	0.6705 (3)	0.4975 (6)	0.4455 (4)	0.0141 (9)
C2	0.7567 (3)	0.6057 (7)	0.6470 (4)	0.0141 (9)
C3	0.8338 (3)	0.4994 (6)	0.5420 (4)	0.0144 (9)
N1	0.6741 (3)	0.5747 (6)	0.5476 (3)	0.0152 (8)
N2	0.7515 (2)	0.4602 (6)	0.4444 (3)	0.0164 (8)
N3	0.8364 (3)	0.5631 (6)	0.6457 (3)	0.0178 (8)
O1	1.0423 (2)	0.8541 (5)	0.5949 (3)	0.0172 (7)
O2	0.7564 (3)	0.6793 (5)	0.7391 (3)	0.0247 (8)
O3	0.9043 (2)	0.4808 (5)	0.5300 (3)	0.0220 (7)
O4	0.5977 (2)	0.4607 (5)	0.3521 (3)	0.0211 (7)
II				
	<i>x</i>	<i>y</i>	<i>z</i>	$U_{\text{iso}}^*/U_{\text{eq}}$
Pb1	1.055927 (15)	1.20519 (3)	0.607963 (18)	0.01807 (11)
Cd1	1.0000	0.75964 (8)	0.7500	0.01442 (14)
C1	0.6796 (4)	0.4848 (7)	0.4601 (5)	0.0167 (11)
C2	0.7726 (4)	0.6294 (8)	0.6594 (5)	0.0183 (11)
C3	0.8509 (4)	0.5198 (8)	0.5485 (5)	0.0189 (11)
N1	0.6852 (3)	0.5750 (7)	0.5626 (4)	0.0187 (10)
N2	0.7629 (3)	0.4541 (7)	0.4563 (4)	0.0191 (10)
N3	0.8550 (3)	0.6037 (7)	0.6523 (4)	0.0196 (10)
O1	1.0410 (3)	0.8666 (6)	0.6050 (3)	0.0166 (8)
O2	0.7742 (3)	0.7108 (6)	0.7513 (4)	0.0244 (9)
O3	0.9212 (3)	0.5042 (6)	0.5329 (4)	0.0246 (9)

O4	0.6037 (3)	0.4306 (6)	0.3697 (3)	0.0209 (8)
----	------------	------------	------------	------------

Table S3. Select bond lengths (Å) and angles (degree) for I and II

I			
Pb1-O1 ⁱ	2.349 (3)	C1-N2	1.374 (5)
Pb1-O1	2.353 (4)	C2-O2	1.247 (5)
Pb1-N1 ⁱⁱ	2.467 (3)	C2-N3	1.361 (6)
Pb2-O1 ⁱⁱⁱ	2.495 (3)	C2-N1	1.372 (6)
Pb2-O1	2.495 (3)	C3-O3	1.253 (6)
Pb2-O4 ^{iv}	2.617 (3)	C3-N3	1.338 (6)
Pb2-O4 ^v	2.617 (3)	C3-N2	1.369 (6)
Pb2-N3	2.637 (4)	C1-O4	1.253 (6)
Pb2-N3 ⁱⁱⁱ	2.637 (4)	C1-N1	1.345 (6)
O4-C1-N1	123.4 (4)	O3-C3-N3	122.0 (4)
O4-C1-N2	119.0 (4)	O3-C3-N2	118.7 (4)
N1-C1-N2	117.6 (4)	N3-C3-N2	119.2 (4)
O2-C2-N3	120.7 (4)	C1-N1-C2	119.8 (4)
O2-C2-N1	117.3 (4)	C3-N2-C1	122.4 (4)
N3-C2-N1	122.0 (4)	C3-N3-C2	118.7 (4)
II			
Pb1-O1 ⁱ	2.319 (4)	C1-N1	1.350 (7)
Pb1-O1	2.389 (4)	C1-N2	1.369 (7)
Pb1-N1 ⁱⁱ	2.545 (4)	C2-O2	1.234 (7)
Cd1-O1 ⁱⁱⁱ	2.266 (3)	C2-N3	1.369 (7)
Cd1-O1	2.266 (3)	C2-N1	1.369 (7)
Cd1-N3	2.302 (5)	C3-O3	1.228 (6)
Cd1-N3 ⁱⁱⁱ	2.302 (5)	C3-N3	1.353 (7)
C1-O4	1.232 (7)	C3-N2	1.381 (8)
O4-C1-N1	123.6 (5)	O3-C3-N3	122.7 (5)
O4-C1-N2	118.5 (5)	O3-C3-N2	119.7 (5)
N1-C1-N2	117.9 (5)	N3-C3-N2	117.6 (5)
O2-C2-N3	120.8 (5)	C1-N1-C2	119.9 (5)
O2-C2-N1	117.5 (5)	C1-N2-C3	123.1 (4)
N3-C2-N1	121.6 (5)	C3-N3-C2	119.7 (5)

References

- (1) Dolabdjian, K.; Ströbele, M.; Meyer, H. J. Crystal Structure of a Commercial Product Called Lead Cyanurate. *Z. Anorg. Allg. Chem.* **2015**, *641*, 765-768.
- (2) Kohn, W. Nobel Lecture: Electronic Structure of Matter-wave Functions and Density Functionals. *Rev. Mod. Phys.* **1999**, *71*, 1253-1266.
- (3) Clark, S. J.; Segall, M. D.; Pickard, C. J.; Hasnip, P. J.; Probert, M. J.; Refson, K.; Payne, M. C. First Principles Methods Using CASTEP. *Z. Kristallogr.* **2005**, *220*, 567-570.
- (4) Liang, F.; Kang, L.; Zhang, X.; Lee, M.; Lin, Z.; Wu, Y. Molecular Construction Using $(\text{C}_3\text{N}_3\text{O}_3)^{3-}$ Anions: Analysis and Prospect for Inorganic Metal Cyanurates Nonlinear Optical Materials. *Cryst. Growth & Des.* **2017**, *17*, 4015-4020.
- (5) Li, Z.; Liang, F.; Guo, Y.; Lin, Z.; Yao, J.; Zhang, G.; Yin, W.; Wu, Y.; Chen, C. $\text{Ba}_2\text{M}(\text{C}_3\text{N}_3\text{O}_3)_2$ (M = Mg, Ca): Potential UV Birefringent Materials with Strengthened Optical Anisotropy Originating from the $(\text{C}_3\text{N}_3\text{O}_3)^{3-}$ Group. *J. Mater. Chem. C* **2018**, *6*, 12879-12887.
- (6) Xia, M.; Zhou, M.; Liang, F.; Meng, X.; Yao, J.; Lin, Z.; Li, R. Noncentrosymmetric Cubic Cyanurate $\text{K}_6\text{Cd}_3(\text{C}_3\text{N}_3\text{O}_3)_4$ Containing Isolated Planar π -Conjugated $(\text{C}_3\text{N}_3\text{O}_3)^{3-}$ Groups. *Inorg. Chem.* **2018**, *57*, 32-36.
- (7) Tang, J.; Liang, F.; Meng, X.; Kang, K.; Yin, W.; Zeng, T.; Xia, M.; Lin, Z.; Yao, J.; Zhang, G.; Kang, B. $\text{Ba}_3(\text{C}_3\text{N}_3\text{O}_3)_2$: A New Phase of Barium Cyanurate Containing Parallel π -Conjugated Groups as a Birefringent Material Replacement for Calcite. *Cryst. Growth & Des.* **2019**, *19*, 568-572.
- (8) Wang, N.; Liang, F.; Yang, Y.; Zhang, S.; Lin, Z. A New Ultraviolet Transparent Hydra-cyanurate $\text{K}_2(\text{C}_3\text{N}_3\text{O}_3\text{H})$ with Strong Optical Anisotropy from Delocalized π -bonds. *Dalton Trans.* **2019**, *48*, 2271-2274.
- (9) Meng, X.; Liang, F.; Kang, K.; Tang, J.; Huang, Q.; Yin, W.; Lin, Z.; Xia, M. A Rich Structural Chemistry in π -conjugated Hydroisocyanurates: Layered Structures of $\text{A}_2\text{B}(\text{H}_2\text{C}_3\text{N}_3\text{O}_3)_4 \cdot n\text{H}_2\text{O}$ (A = K, Rb, Cs; B = Mg, Ca; n = 4, 10) with High Ultraviolet Transparency and Strong Optical Anisotropy. *Dalton Trans.* **2019**, *48*, 9048-9052.
- (10) Meng, X.; Liang, F.; Tang, J.; Kang, K.; Huang, Q.; Yin, W.; Lin, Z.; Xia, M. $\text{Cs}_3\text{Na}(\text{H}_2\text{C}_3\text{N}_3\text{O}_3)_4 \cdot 3\text{H}_2\text{O}$: A Mixed Alkali-Metal Hydroisocyanurate Nonlinear Optical Material Containing π -Conjugated Six-Membered-Ring Units. *Eur. J. Inorg. Chem.* **2019**, *2019*, 2791-2795.
- (11) Meng, X.; Liang, F.; Tang, J.; Kang, K.; Zeng, T.; Yin, W.; Guo, R.; Lin, Z.; Xia, M. Parallel Alignment of π -Conjugated Anions in Hydroisocyanurates Enhancing Optical Anisotropy. *Inorg. Chem.* **2019**, *58*, 8948-8952.
- (12) Liang, F.; Wang, N.; Liu, X.; Lin, Z.; Wu, Y. Co-crystal $\text{LiCl} \cdot (\text{H}_3\text{C}_3\text{N}_3\text{O}_3)$: A Promising Solar-blind Nonlinear Optical Crystal with Giant Nonlinearity From Coplanar π -conjugated Groups. *Chem. Commun.* **2019**, *55*, 6257-6260.
- (13) Perdew, J. P.; Burke, K.; Ernzerhof, M. Generalized Gradient Approximation Made Simple. *Phys. Rev. Lett.* **1996**, *77*, 3865-3868.
- (14) Vanderbilt, D. Soft Self-consistent Pseudopotentials in a Generalized Eigenvalue Formalism. *Phys. Rev. B* **1990**, *41*, 7892-7895.
- (15) Monkhorst, H. J.; Pack, J. D. Special Points For Brillouin-Zone Integrations. *Phys. Rev. B* **1976**, *13*, 5188-5192.